in: *The International GNSS Service (IGS): Perspectives and Visions for 2010 and beyond, IGS Tech. Rept.*, 8 pp., Darmstadt, 2006.

Rapid Determination of Earthquake Magnitude using GPS for Tsunami Warning Systems: An Opportunity for IGS to Make a Difference

Geoffrey Blewitt,[1] Corné Kreemer,[1] William C. Hammond,[1] Hans-Peter Plag,[1]
Seth Stein,[2] and Emile Okal[2]

[1]Nevada Bureau of Mines and Geology, and Seismological Laboratory, University of Nevada, Reno, Nevada, USA. (gblewitt@unr.edu)
[2]Department of Geological Sciences, Northwestern University, Evanston, Illinois, USA.

Abstract

IGS has an opportunity to contribute to future tsunami warning systems around the globe. This would require real-time access to IGS data and precise GPS orbit and clock information, and software to analyze these data in real time. In a recent study [*Blewitt et al.*, 2006] we showed that current 30 second data from the existing IGS network would have been sufficient to identify the extreme oceanwide tsunami danger of the 26 December 2004 Sumatra earthquake within 15 minutes of earthquake initiation. To assess design requirements we test the effect of adding near-field stations, and of the quality of real-time orbits and clocks. We find that orbit accuracy is of paramount importance, coupled with the need for more IGS stations near subduction zones. A higher data rate is also likely to improve sensitivity, but is of secondary importance.

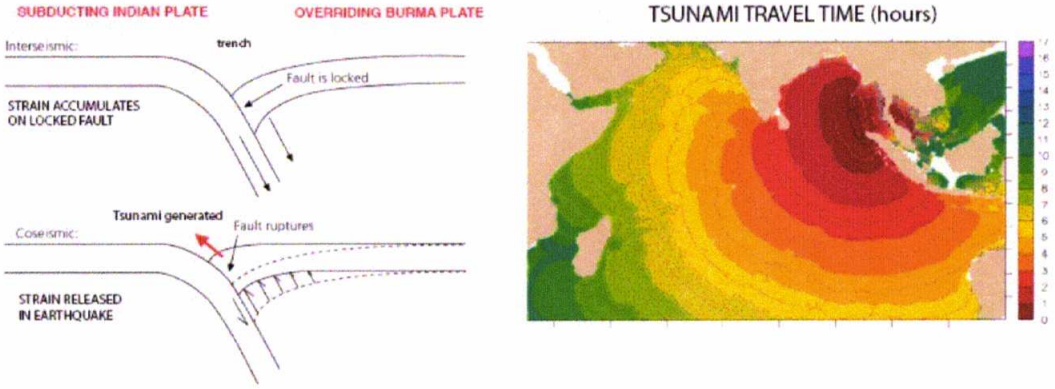

Figure 1. (Left) Tectonic mechanism for generating tsunamis at submarine subduction zones. (Right) Travel time for the oceanwide tsunami ensuing from the 2004 Sumatra earthquake [*PMEL*, 2005].

1. Introduction

The 26 December 2004 Sumatra earthquake (M_w 9.2–9.3) generated the most deadly tsunami in history. Yet within the first hour, the true danger of a major oceanwide tsunami was not indicated by seismic magnitude estimates, which were far too low (M_w 8.0–8.5) [*Kerr*, 2005]. This problem relates to the inherent saturation of early seismic-wave methods. In a recent study [*Blewitt et al.*, 2006] we analyzed 30-s data from the existing IGS network and showed that the earthquake's true size and tsunami potential could be determined using data up to only 15 min after earthquake

initiation, by tracking the permanent displacement of GPS stations associated with the arrival of seismic waves. Within minutes, displacements of >10 mm are detectable as far away as India, consistent with results using weeks of data after the event. These displacements imply M_w 9.0 ± 0.1, indicating a high tsunami potential. This suggests existing GPS infrastructure could be developed into an effective component of tsunami warning systems.

In this paper we summarize *Blewitt et al.* [2006] and discuss the potential for IGS to contribute to a GPS component of future tsunami warning systems based on this technique. Specifically, we draw conclusions on the importance of GPS network configuration, we make a preliminary investigation into the requirements of real-time orbit determination, and we consider possible alternatives for future IGS products that could be applied.

2. Oceanwide Tsunami Warning and Earthquake Magnitude

Tsunamis are gravitational oscillations of the ocean, which can be generated by the rapid displacement of the ocean floor at the trench associated with fault slip during an earthquake (Figure 1). Part of the tsunami moves toward the shore (hitting within ~10 minutes or so) and tanother moves in the opposite direction across the ocean. Such oceanwide tsunamis can take up to a few hours to reach distant shores, moving at the speed of a jet aircraft. These oceanwide tsunamis typically require very great earthquakes of moment magnitude $M_w > 8.5$, thus it is important to be able to identify such great earthquakes quickly (within much less than 1 hour) with minimal chance of a false alarm.

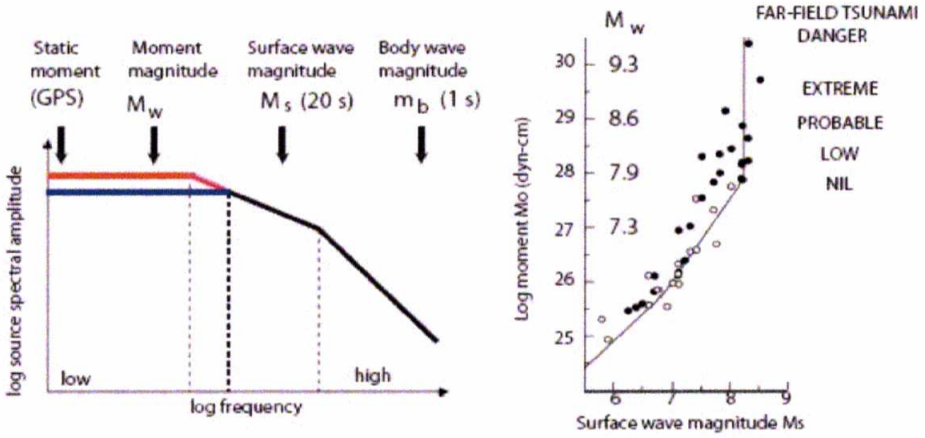

Figure 2. (Left) Illustration of earthquake spectra showing corner frequencies (dashed vertical lines) and different magnitude determinations. The earthquake whose spectrum is shown in red has larger moment magnitude than the one with spectrum shown in blue, even though they have the same surface and body wave magnitudes, as shown by the black part of the spectra that are the same for both earthquakes. GPS samples the lowest frequency part of the spectrum, and as a time-domain measurement system, can readily sample static offsets. (Right) Due to surface wave magnitude saturation, earthquakes of the same Ms can have very different seismic moments [*Geller*, 1976] and thus risk of generating an oceanwide tsunami

During a great submarine earthquake, the ocean floor moves so rapidly that the ocean cannot respond initially except to move *en masse* along with the vertical motion of the ocean floor, so that

the sea surface approximately follows the shape of the deformed ocean floor. Hence the tsunami potential of an earthquake is closely related to its seismic moment $M_0 = \mu sA$ (where μ is rigidity, s is the mean slip on the fault, and A is the area of the fault). M_0 is often reported on a logarithmic scale in terms of the moment magnitude M_w [*Hanks and Kanamori*, 1979]. Thus, of the various earthquake magnitudes that can be computed from seismic observations, M_w is the most appropriate to assess tsunami potential, but is the most difficult to determine quickly because most seismological techniques are sensitive to the shorter period components (Figure 2). This was the case for the 2004 Sumatra event, where the initial seismological magnitude estimate of about 8.0 grossly underestimated its size. It took almost 5 hours before the Harvard Centroid Moment Tensor (CMT) Project adapted its computation to use longer period (300-s versus the standard 135-s) surface waves to infer M_w 9.0, for which the tsunami risk would be very high.

Real-time tsunami models under development are based on the physics of ocean wave propagation and are initialized by an earthquake source [*Titov*, 2005]. By far the most important parameters for the prediction of *oceanwide* tsunami wave heights in the far field are the moment magnitude and the (distributed) earthquake location [*Titov*, 2005]. Seismology can locate the epicenter -- where the rupture starts -- within minutes with sufficient accuracy. *Blewitt et al.* [2006] showed that, given this information, GPS can then be used to determine the moment magnitude, and the location of the extended source. Inversion of GPS displacements results in an earthquake model that predicts the vertical displacement of the ocean floor. This suggests that GPS is particularly well-suited as a technique to initialize real-time tsunami models.

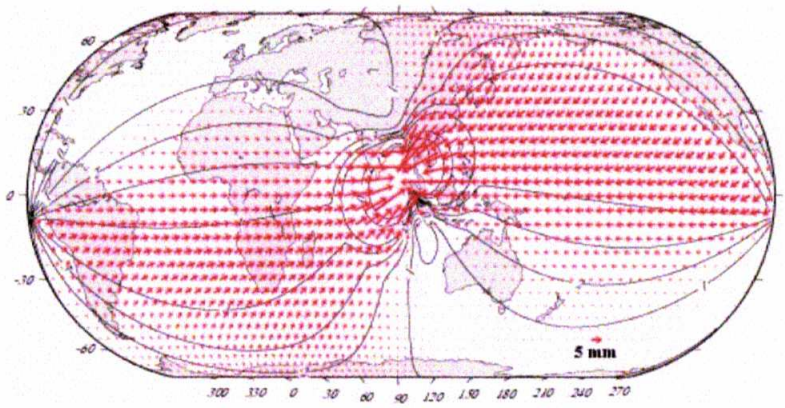

Figure 3. Displacement field of the Sumatra earthquake by inverting IGS data [*Kreemer et al.*, 2006].

3. Permanent Surface Displacements using IGS Data

Permanent displacements of the Earth's surface determined by GPS can be used to constrain earthquake models from which M_0 and hence M_w can be computed. When using GPS, M_0 is often called the "static moment", which equals the seismic moment if the fault ruptures entirely seismically. GPS estimates of the Sumatra earthquake's static moment (using IGS data from days to weeks around the time of the event) correspond to M_w 9.0–9.2 [*Banerjee et al.*, 2005; *Vigny et al.*, 2005; *Kreemer et al.*, 2006], consistent with longest period seismology [*Stein and Okal*, 2005;

Park et al., 2005]. Inverted models of the Sumatra earthquake predicts permanent displacements of millimeters globally (Figure 3), and >10 mm as far away as India at 2000 km from the epicenter. These permanent displacements appear as offsets in the daily station coordinate time series (Figure 4). To be useful for tsunami warning systems, these offsets would have to be resolved accurately using much less than 1 hr of data following the start of the event.

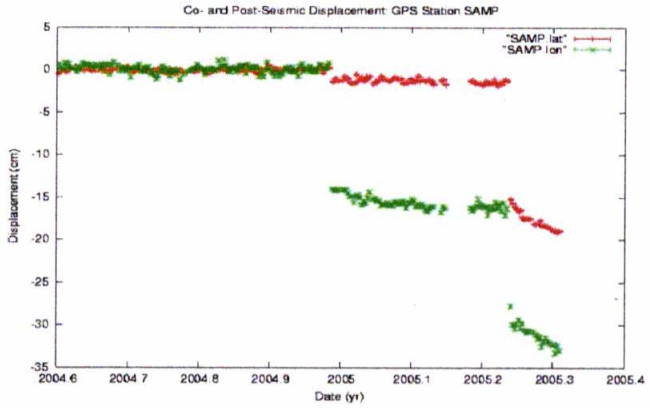

Figure 4. Daily time series of horizontal coordinates for station SAMP (Indonesia), showing co- and post-seismic displacements for the 2004 Sumatra earthquake and 2005 Nias earthquake.

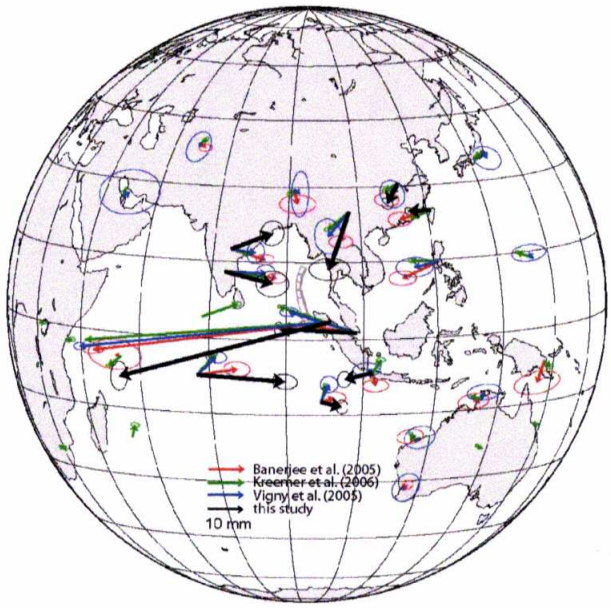

Figure 5. Displacement solutions (black) using only data up to 15 minutes after the earthquake origin time, compared with various published results using data from days to weeks after the event.

Blewitt et al. [2006] processed 30-sec data from the IGS network using JPL's GIPSY-OASIS II software to estimate the static displacements using only data up to 15 min after the earthquake origin time and then used these displacements constrain M_w starting only with knowledge of the earthquake epicenter from near-real time seismology. Station positions were estimated in two

categories: (1) in order to provide a stable reference frame, the 28 far-field station positions (> 3500 km from the epicenter) were estimated as constants over the 24-hr period, and (2) in order to determine surface displacements to invert for earthquake parameters, the 10 near- to mid-field station positions were estimated independently at every 30-s epoch. In addition, the station coordinate time series were calibrated to mitigate carrier phase multipath error, which approximately repeats every sidereal day [*Genrich and Bock*, 1992; *Choi et al.*, 2004]. This calibration was computed using a position-based sidereal filter, by stacking the 30-s epoch coordinate time series from the previous 4 days, shifting each series by 4 min per day. The actual processing time for a 38-station network is ~15% of real time on an ordinary 1-cpu PC running Linux, thus posing no fundamental problem for real-time implementation. The resulting estimated displacements (Figure 5) agree to 7 mm RMS with published estimates [*Banerjee et al.*, 2005; *Vigny et al.*, 2005; *Kreemer et al.*, 2006] that were based on weeks of post-earthquake data. The resulting near-real time earthquake model predicts displacements that agree to 4 mm RMS with published models.

4. Effect of Real-Time Orbit Quality

Blewitt et al. [2006] applied the above procedure where simultaneously estimated parameters included satellite orbit state vectors (initialized using the Broadcast Ephemeris acquired prior to the earthquake), stochastic solar radiation pressure on the satellites, satellite and station clocks at every 30-s epoch, the Earth's pole position and drift rate, the Earth's rate of rotation, random-walk variation in zenith tropospheric delay and gradients at each station, carrier phase biases and cycle slips, and station positions. Here we also test alternative options for real time orbits, including the Broadcast Ephemeris, and the IGS Ultra-Rapid orbits. In all cases, satellite clocks were estimated as white noise at every epoch (equivalent to double differencing).

The IGS ultra rapid orbits are published 4 times per day, each with an initial latency of 3 hours. As a consequence, the actual latency in real time falls in the range 3-9 hours. In this particular case, the latency was 7 hours, meaning that the orbits were actually predicted ahead 7 hours until the time of the earthquake. To test whether the systematic drifts evident in Figure 6 (Bottom) were due to errors in prediction, we also tested the IGS ultra-rapid orbits published 6 hours later, with 1 hour latency. Very similar drifts were evident, thus prediction does not appear to be the main cause of the drifts.

To test the performance of the IGS rapid orbits, we followed the procedure detailed in Blewitt et al., [2006] to estimate displacements from the time series (with a 15 minute deadline) and then computed the goodness of fit χ_v^2 for the entire variety of northward rupturing models with a range of M_w 8.0–9.5 (Figure 7). An F-statistic was computed relative to the best-fitting model to assess the range of M_w for models that are not significantly different in quality than the best-fitting model. The results were then compared to those for the estimated orbits presented in Blewitt et al. [2006].

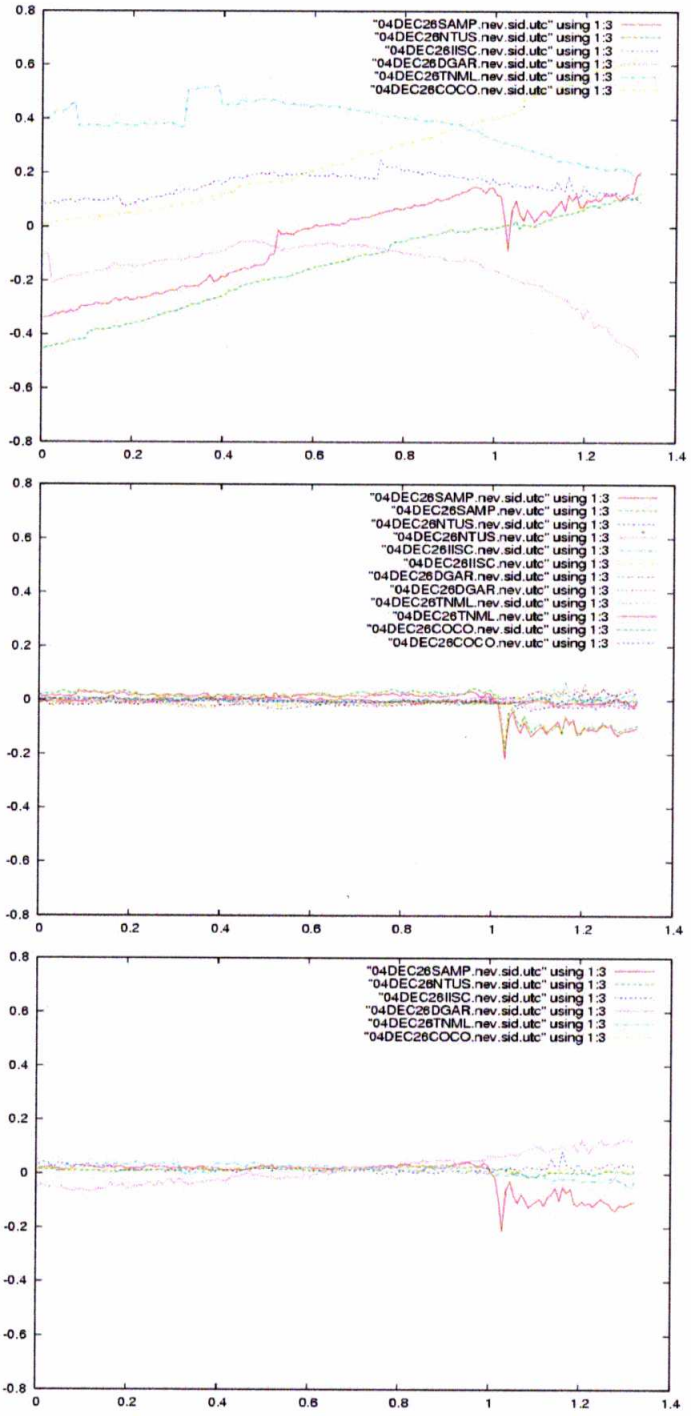

Figure 6. Coordinate time series (30 sec) on 26 December 2004 using (Top) Broadcast Ephemeris, (Middle) estimated orbits, and (Bottom) IGS ultra-rapid orbits. In all cases, satellite clocks were estimated. The resulting time series (Figure 6) show that solutions using the Broadcast Ephemeris are dominated by systematic drifts and jumps. In contrast time series using estimated orbits are very flat until the seismic waves arrive each station (at ~01:00 UTC), after which the stations are permanently displaced. *Blewitt et al.* [2006] shows each time series in more detail. The IGS ultra-rapid orbits produce results with slight systematic drifts as compared to the case using estimated orbits.

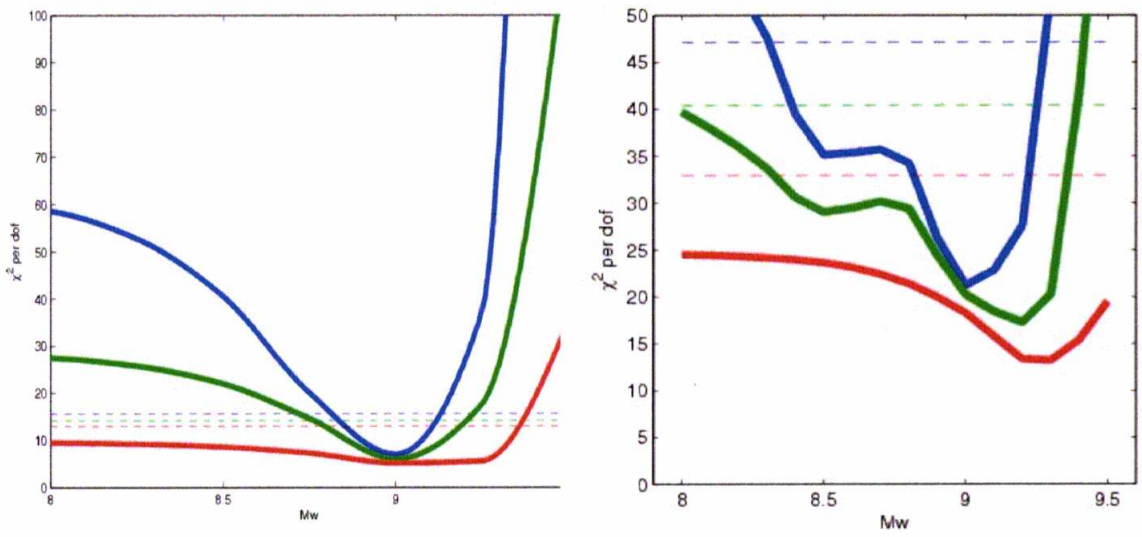

Figure 7. Reduced chi-square χ_v^2 summarizing the misfit of displacements as a function of M_w (Left) using estimated orbits *[Blewitt et al.*, 2006]; (Right) using IGS ultra-rapid orbits. For each plot, three cases are shown: all stations (blue), all except nearest (300 km) station SAMP (green), and all except SAMP and next nearest (900 km) station NTUS (red). The dashed lines indicate 95% confidence intervals.

Whereas for the estimated orbits M_w is constrained with 95% confidence to the range 8.8–9.1, for the IGS ultra rapid orbits M_w is only constrained to the range 8.3-9.3. As it stands, the results for the IGS ultra rapid orbits are not sufficiently precise for purposes of tsunami warning, because of the problem of false alarms. One possible way forward is to modify the displacement estimation algorithm by estimating a low-order polynomial to the time series, though this has not been attempted here. A more robust way forward is to install more sites in the near field. Figure 7 once again confirms that near-field sites are critical to constrain the range of earthquake models. Fortunately, many such sites are being installed for scientific purposes, and so could be included in the IGS by making timely data available.

5. Conclusions

We have shown that the magnitude, mechanism, and spatial extent of rupturing of the 26 December 2004 Sumatra earthquake can be accurately determined using only 15 min of 30-sec GPS data following earthquake initiation, using data from existing IGS network. Most importantly, the GPS method would have clearly ruled out the earliest misleading indications from seismology that there was little danger of a major oceanwide tsunami. This method would be applicable to the class of greatest submarine earthquakes of moment magnitude >8.5.

The method works best if orbits are estimated simultaneously with station coordinate time series, though the use of IGS ultra rapid orbits also looks promising. The method only works with stations in the near field of the earthquake (< 1 rupture length). The range of possible earthquake models can be more tightly constrained by the installation of more GPS stations in the near field.

Thus the IGS has an opportunity to make a difference to warning systems for far-field (oceanwide) tsunamis. Important steps for IGS to take are (1) make all data from the IGS network available in real time, (2) densify the IGS network near subduction zones, (3) work toward improving IGS ultra rapid orbits and clocks, and (4) make available "standard" software to compute precise point positions in real time, consistent with the IGS products. Taking these steps would allow for the implementation of a near real-time system that could estimate the critical parameters for far-field tsunami prediction, which are the seismic moment and the extended location of the source [*Titov et al.*, 2005].

Acknowledgments. This work was supported in part by NASA Interdisciplinary Science and NASA Solid Earth and Natural Hazards.

References

Banerjee, P., F. Pollitz, and R. Burgmann (2005), The size and duration of the Sumatra-Andaman earthquake from far-field static offsets, *Science, 308*, 1769-1772.

Blewitt, G., C. Kreemer, W. Hammond, H.-P. Plag, S. Stein, and E. Okal (2006), Rapid determination of earthquake magnitude using GPS for tsunami warning systems, Geophys. Res. Lett., L11309, doi:10.1029/2006GL026145.

Choi, K., A. Bilich, K. Larson, and P. Axelrad (2004), Modified sidereal filtering: Implications for high-rate GPS positioning, *Geophys. Res. Lett., 31*, L22608, doi:10.1029/2004GL021621.

Geller, R.J. (1976), Scaling relations for earthquake source parameters and magnitudes, *Bull. Seismol. Soc. Am., 66*, 1501-1523.

Genrich, J. and Y. Bock (1992), Rapid resolution of crustal motion at short ranges with the Global Positioning System, *J. Geophys. Res., 97*, 3261-3269.

Kreemer, C., G. Blewitt, W. Hammond, and H.-P. Plag (2006), Global deformation from the great 2004 Sumatra-Andaman earthquake observed by GPS: Implications for rupture process and global reference frame, *Earth Planets and Space, 58*, 141-148.

Hanks, T., and H. Kanamori (1979), A moment magnitude scale, *J. Geophys. Res., 84*, 2348-2350

Kerr, R. A. (2005), Failure to gauge the quake crippled the warning effort, *Science, 307*, 201.

PMEL (2005), http://nctr.pmel.noaa.gov/index.html.

Park, J. *et al.* (2005), Earth's free oscillations excited by the 26 December 2004 Sumatra-Andaman earthquake, *Science, 308*, 1139-1144.

Stein, S. and E. Okal (2005), Speed and size of the Sumatra earthquake, *Nature 434*, 581-582.

Titov, V., F. González, E. Bernard, M. Eble, H. Mofjeld, J. Newman, and A. Venturato (2005), Real-time tsunami forecasting: challenges and solutions, *Natural Hazards 35*, 41-58.

Vigny C., *et al.* (2005), Insight into the 2004 Sumatra-Andaman earthquake from GPS measurements in Southeast Asia, *Nature, 436*, 201-206.